



**HAL**  
open science

## **A Novel Antibacterial Compound Decreases MRSA Biofilm Formation Without the Use of Antibiotics in A Murine Model**

Houssam Bouloussa, Zoe Durand, Emmanuel Gibon, Antonia F. Chen, Matthew Grant, Azzam Saleh-mghir, Mohsin Mirza, Bradley Stutzman, Claudio Vergari, James Yue, et al.

► **To cite this version:**

Houssam Bouloussa, Zoe Durand, Emmanuel Gibon, Antonia F. Chen, Matthew Grant, et al.. A Novel Antibacterial Compound Decreases MRSA Biofilm Formation Without the Use of Antibiotics in A Murine Model. *Journal of Orthopaedic Research*, 2023, 10.1002/jor.25638 . hal-04195338

**HAL Id: hal-04195338**

**<https://hal.science/hal-04195338>**




Submitted on 4 Sep 2023

**HAL** is a multi-disciplinary open access archive for the deposit and dissemination of scientific research documents, whether they are published or not. The documents may come from teaching and research institutions in France or abroad, or from public or private research centers.

L'archive ouverte pluridisciplinaire **HAL**, est destinée au dépôt et à la diffusion de documents scientifiques de niveau recherche, publiés ou non, émanant des établissements d'enseignement et de recherche français ou étrangers, des laboratoires publics ou privés.

## RESEARCH ARTICLE

# A novel antibacterial compound decreases MRSA biofilm formation without the use of antibiotics in a murine model

Houssam Bouloussa<sup>1</sup> | Zoe Durand<sup>1</sup> | Emmanuel Gibon<sup>1</sup>  | Antonia F. Chen<sup>2</sup>  | Matthew Grant<sup>3</sup> | Azzam Saleh-Mghir<sup>4</sup> | Mohsin Mirza<sup>1</sup> | Bradley Stutzman<sup>5</sup> | Claudio Vergari<sup>6</sup>  | James Yue<sup>7</sup> | Nelson Anzala<sup>8</sup> | Dorian Bonnot<sup>8</sup> | Sandrine Albac<sup>8</sup> | Othman Bouloussa<sup>5</sup> | Delphine Croisier<sup>8</sup>

<sup>1</sup>DeBogy Molecular Inc., Farmington, Connecticut, USA

<sup>2</sup>Department of Orthopaedic Surgery, Brigham and Women's Hospital, Harvard Medical School, Boston, Massachusetts, USA

<sup>3</sup>Section of Infectious Diseases, New Haven, Connecticut, USA

<sup>4</sup>UVSQ-Inserm, UMR 1173 Infection and Inflammation, Montigny-le-Bretonneux, France

<sup>5</sup>Technology Incubation Program, Farmington, Connecticut, USA

<sup>6</sup>Arts et Métiers Sciences et Technologie, Institut de Biomécanique Humaine Georges Charpak, Paris, France

<sup>7</sup>CT Orthopaedic Specialists, Department of Surgery, Frank H Netter School of Medicine Quinnipiac University, North Haven, Connecticut, USA

<sup>8</sup>Vivexia SARL, Dijon, France

## Correspondence

Houssam Bouloussa, DeBogy Molecular Inc., 400 Farmington Ave, Farmington, CT 06032, USA.

Email: [houssam.bouloussa@debogy.com](mailto:houssam.bouloussa@debogy.com)

## Abstract

Despite significant advancements in material science, surgical site infection (SSI) rates remain high and prevention is key. This study aimed to demonstrate the in vivo safety and antibacterial efficacy of titanium implants treated with a novel broad-spectrum biocidal compound (DBG21) against methicillin-resistant *Staphylococcus aureus* (MRSA). Titanium (Ti) discs were covalently bound with DBG21. Untreated Ti discs were used as controls. All discs were implanted either untreated for 44 control mice or DBG21-treated for 44 treated mice. After implantation,  $1 \times 10^7$  colony forming units (CFU) of MRSA were injected into the operating site. Mice were killed at 7 and 14 days to determine the number of adherent bacteria (biofilm) on implants and in the peri-implant surrounding tissues. Systemic and local toxicity were assessed. At both 7 and 14 days, DBG21-treated implants yielded a significant decrease in MRSA biofilm (3.6 median  $\log_{10}$  CFU [99.97%] reduction [ $p < 0.001$ ] and 1.9 median  $\log_{10}$  CFU [98.7%] reduction [ $p = 0.037$ ], respectively) and peri-implant surrounding tissues (2.7 median  $\log_{10}$  CFU/g [99.8%] reduction [ $p < 0.001$ ] and 5.6 median  $\log_{10}$  CFU/g [99.9997%] reduction [ $p < 0.001$ ], respectively). There were no significant differences between control and treated mice in terms of systemic and local toxicity. DBG-21 demonstrated a significant decrease in the number of biofilm bacteria without associated toxicity in a small animal implant model of SSI. Preventing biofilm formation has been recognized as a key element of preventing implant-related infections.

## KEYWORDS

biofilm, implants, infection, prevention, titanium

This is an open access article under the terms of the Creative Commons Attribution License, which permits use, distribution and reproduction in any medium, provided the original work is properly cited.

© 2023 DeBogy Molecular, Inc, Vivexia and The Authors. *Journal of Orthopaedic Research*® published by Wiley Periodicals LLC on behalf of Orthopaedic Research Society.

## 1 | INTRODUCTION

Bacterial infections, especially when associated with biofilm, represent one of the most serious complications following the implantation of medical devices.<sup>1</sup> Surgical-site infections (SSIs) and periprosthetic joint infections (PJIs) are particularly devastating for orthopaedic patients as antibiotics have difficulty reaching dormant bacteria in low-nutrient microenvironments such as implant surfaces and bone.<sup>2</sup> Biofilm is an exopolysaccharidic matrix comprised of bacteria with reduced antibiotic sensitivity and poor mechanical accessibility. Biofilm formation plays a central role in the failure of conservative treatments (debridement, antibiotics, irrigation, and implant retention) for implant-related infections.<sup>3</sup> Preventing biofilm formation has been recognized as a key element of SSI and implant-related infection prevention. Yet, in most medical disciplines, nothing new has been implemented in clinical practice that effectively reduces biofilm formation at the surface of implants. Bacterial biofilm is strongly associated with failure of infection control, infection recurrence, and the development of chronic infections.<sup>4</sup>

The emergence of antibiotic-resistant bacterial strains has pushed for the development of nonselective antibacterial coatings and next-generation innovative solutions.<sup>5</sup> Those attempts have been unsuccessful at translating from the bench to the bedside to date. Most of these technologies, though interesting at the academic level, have not become mainstream in the industry due to concerns over safety (silver agents), transient efficacy (antibiotic-leaching compounds), or scalability (multistep processes, in situ polymerization meaning that coatings are produced by a chemical reaction in contact with the implant surface, which is suboptimal for the industry).<sup>6-13</sup> Nanostructured surfaces aimed at preventing bacterial adhesion are not bactericidal and therefore, display a low efficacy in preventing the emergence of biofilm in vivo.<sup>14</sup> Ideally, a permanent surface modification that would be both antibacterial and biocompatible would reduce the incidence of implant-related infection and make implant removals unnecessary. Surface modification of implants is superior to coatings in terms of stability and durability, since coatings tend to scale off with time, while surface modification relies on covalent bonding of compounds on the target substrate.<sup>15</sup> This is the rationale behind the clinical need for permanent antimicrobial protection of surfaces which transient eluting coatings cannot fully address.

An ideal antimicrobial surface protection should be able to support the following claims: prevention of implant-related infection, long-lasting protection of implant surfaces from late onset bacterial hematogenous spread, indirect decrease of surrounding tissue bacterial load by drastic biofilm inhibition, excellent local and systemic biocompatibility profile, stability (no release of potentially toxic compounds), full sterilizability, scalability, cost-effectiveness, and no alteration of bone ingrowth. Therefore, a novel ready-to-use antimicrobial compound (DBG21) graftable on titanium-alloy implants (Ti-6Al-4V) was developed with the goal to form a permanently modified surface that would inhibit the growth of biofilm. DBG21 is a bifunctional polymer that has both the ability to

covalently bind to surfaces and to eliminate bacteria. To proceed with a preclinical assessment, the objectives of this study were (1) to assess safety (local and systemic toxicity study of treated surfaces versus nontreated surfaces implanted subcutaneously in mice in the absence of infection); (2) to assess the antibacterial efficacy of treated implant surfaces versus nontreated implant surfaces using a previously validated MRSA subcutaneous infection murine model; (3) to provide pathology data on the peri-implant tissue response in the setting of the same infection murine model.

## 2 | METHODS

### 2.1 | Animals

A total of 88 BALB/c mice (11-week-old, 22–24 g) were used (Charles River, France) for the entire study (Table 1). These animals were housed in a protected area at the small animal facility of the University of Burgundy, Dijon, France (Biosafety level 2 facility) and were fed ad libitum according to the current recommendations of the European Institute of Health. No fasting was required for this study. Before each experiment, animals were housed for 1 or 2 weeks at the animal facility. During this period and for the duration of the study, qualified staff members checked on animals twice a day and assessed their well-being. The animal facility was authorized by the French authorities (Agreement N° C 21 464 04 EA). Animal housing and experimental procedures were conducted according to the French and European Regulations and NRC Guide for the Care and Use of Laboratory Animals. All procedures using animals were submitted to the Animal Care and Use Committee C2EA accredited by the French authorities (APAFIS #33499-2021101914348582).

**TABLE 1** Summary of groups.

	N	Inoculum size (CFU/mouse)	Purpose	Day of autopsy
<b>Treated group</b>				
Total	44			
Studies	18	10 <sup>7</sup>	Efficacy	D7
	3	10 <sup>7</sup>	Pathology	
	5	N/A	Tolerance	D11
	15	10 <sup>7</sup>	Efficacy	D14
	3	10 <sup>7</sup>	Pathology	
<b>Control group</b>				
Total	44			
Studies	18	10 <sup>7</sup>	Efficacy	D7
	3	10 <sup>7</sup>	Pathology	
	5	N/A	Tolerance	D11
	15	10 <sup>7</sup>	Efficacy	D14
	3	10 <sup>7</sup>	Pathology	

## 2.2 | Bacterial strains and culture conditions

A methicillin-resistant *Staphylococcus aureus* (MRSA) (ATCC 43300) strain was kept at  $-80^{\circ}\text{C}$  in cryobeads (bioMérieux, France). The strain was streaked on Chapman agar plate (bioMérieux) and cultured for 18 h at  $37^{\circ}\text{C}$ . A single colony was used to inoculate 9 mL into brain heart infusion (BHI, bioMérieux) under agitation for 6 h at  $37^{\circ}\text{C}$ . This bacterial culture was in turn used to inundate a Mueller-Hinton (MH) agar plate (bioMérieux) that was incubated for 18 h at  $37^{\circ}\text{C}$ . The following day, the MH agar plate was scraped into 10 mL saline (in the presence of glass beads to prevent the formation of clumps) and vortexed to obtain a solution at  $2 \times 10^{10}$  CFU/mL. Successive dilutions were performed to obtain the target inoculum size and the bacterial load was determined following plating of the dilutions on MH agar plates.

## 2.3 | Titanium-alloy implants

Forty-four Ti-6Al-4V discs, 6 mm  $\varnothing$ , 0.5 mm thick, were sonicated in pure ethanol for 10 min to remove impurities, air-dried, activated, dip-coated in an ethanolic polymer solution (proprietary DBG21 high-density quaternary ammonium polymer, DeBogy Molecular Inc.) and heated at  $130^{\circ}\text{C}$  for 3 h to produce covalently bound DBG21-treated discs. All the unbound polymer was removed by sonicating DBG21-treated discs in pure ethanol for 30 min. Discs were then air-dried. Forty-four control Ti-6Al-4V discs underwent the same activation process without being treated with the polymer solution. All discs were individually stored in double peel packs. Following packaging, all discs underwent subsequent sterilization by 25 kGy irradiation using a Cobalt-60 gamma irradiator (VPT Rad).

## 2.4 | Tolerance study

The experimental model was performed as previously described.<sup>16</sup> Briefly, mice were anesthetized by an intraperitoneal (IP) injection of a mix of ketamine (50 mg/kg) (Virbac) and xylazine (10 mg/kg) (Bayer HealthCare). The flank on the right side was shaved and then disinfected by three consecutive applications of betadine/sterile water. A cutaneous incision of 0.5 cm was made under sterile conditions and an untreated implant (control) or a treated implant (DBG21-treated) was subcutaneously inserted and placed at about 2 cm from the incision site. Five mice received an untreated implant (control) and five mice received a treated implant. The incision was sutured and disinfected once a day for 3 days after surgery. Based on the ISO 10993-11:2017 standard,<sup>17</sup> systemic acute and subacute toxicity was evaluated in mice receiving DBG21-treated implants compared to mice receiving untreated implants (controls) in the absence of infection. These mice were monitored daily over an 11-day period (weight, daily clinical score). Clinical scoring (ISO 10993-11:2017 standard<sup>17</sup>) included: movement, body posture, fur quality, degree of eye opening, body weight. At Day 11, blood samples were

collected through intracardiac puncture on all animals previously anesthetized via a mix of ketamine and xylazine. Euthanasia was performed immediately after the intracardiac puncture by cervical dislocation. A blood biochemical analysis included urea, creatinine, protein, albumin, liver function tests (alkaline phosphatase, alanine aminotransferase, glutamate dehydrogenase, total bilirubin), electrolytes ( $\text{Na}^+$ ,  $\text{K}^+$ ,  $\text{Cl}^-$ ) and glucose. Blood was collected into purple-top potassium EDTA tubes and stored at  $4^{\circ}\text{C}$  until shipment. The relevant tubes were sent to Cerbavet (Massy) for analysis and results were available within 24 h.

## 2.5 | Efficacy study

The surgical insertion of implants was performed as described above. Immediately after disc implantation, an inoculum of 100  $\mu\text{L}$  ( $1 \times 10^7$  CFU/mouse of ATCC 43300 MRSA strain) of the bacterial culture was injected onto the implant. Mice received either an untreated implant or a DBG21-treated implant. The day of infection was referred to as D0. At Day 7 (D7), 36 mice (18 control mice, 18 treated mice) were killed by cervical dislocation performed under anesthesia. The implant was collected and then used for bacterial enumeration. At D14, the same procedure was repeated with the 30 remaining mice (15 control mice, 15 treated mice). Histopathological analysis was performed in three additional mice of each group since histopathological analysis and microbiological enumeration cannot be performed in the same mice.

## 2.6 | Investigation of biofilm on implants and CFU<sub>s</sub> in surrounding tissues

### 2.6.1 | Bacterial load on implants

Each implant was individually washed under aseptic conditions in an Eppendorf tube (three successive washing steps with 300, 400, and 500  $\mu\text{L}$  of sterile saline). After the last wash, the implant was suspended into 1 mL of sterile saline, placed into an ultrasonic bath (AdvantageLab) for 3 min at room temperature before being vigorously vortexed to detach all adherent bacteria from the implant. Several successive dilutions of this suspension (undiluted,  $10^{-2}$ ,  $10^{-4}$ ) were then cultured onto Chapman agar plates for 24–48 h at  $37^{\circ}\text{C}$ . If required, dilutions were repeated in case of unconvincing or inadequate results, the stability of the suspension at  $4^{\circ}\text{C}$  for 48 h having been previously verified. The limit of detection was determined as being 1 log<sub>10</sub> CFU on implants.

### 2.6.2 | Bacterial load in surrounding tissues

Adjacent tissue (mostly subcutaneous fat and occasional muscle fibers) of each implant were dissected, weighed, resuspended into 1 mL of saline solution and homogenized using a bead beating grinder and lysis system (FastPrep-24 5G, MP Biomedical; 1 cycle of 30 s at 4 m/s with 1 ceramic beads). Crushed tissues were serially diluted down to  $10^{-6}$

and 10  $\mu\text{L}$  of each dilution was plated by spotting-and-tilt-spreading (SATS) approach on Chapman agar plates. The limit of detection was determined as being 1  $\log_{10}$  CFU/g of surrounding tissues.

### 2.6.3 | Pathology analysis

During the necropsy at D7 and D14 postimplantation for infected mice and D11 for noninfected mice, the tissue surrounding the implant was excised from animals and then kept in a histological cassette to avoid distortion of the sample and fixed in 10% formaldehyde. All samples (22 subcutaneous murine tissue specimens with titanium implants and apical orientation sutures) were then sent for paraffin-embedding and further histological analysis (Haematoxylin/Eosin/Saffron staining) to Atlantic Bone Screen (Saint-Herblain). The samples (subcutaneous tissue with the titanium implant) were processed at Atlantic Bone Screen. The samples were stored at room temperature in a dedicated location until the start of the experiments. The titanium discs were removed, and the tissue samples were embedded in paraffin and stained with Haematoxylin/Eosin/Saffron. For each block, sections of 3–4  $\mu\text{m}$  were made and placed on Superfrost slides. The slides were dried under a fume hood overnight at room temperature before being used for HES staining. The quality of the histological sections present on each slide was individually assessed before any processing. Similarly, the quality of each staining was individually checked at the end of the procedure. A veterinary pathologist further performed the histological analysis of the produced microscopic slides (graduate of the European College of Veterinary Pathologists). The veterinary pathologist separately documented, illustrated, and commented on any notable events.

### 2.6.4 | Microscopic examination

All samples (corresponding to a total of 22 sections, 10 from mice used in the tolerance study and 12 from mice in the antibacterial efficacy study) were observed by a veterinarian pathologist in a blinded fashion. All significant events were listed, recorded, and documented. Studied parameters were inflammation, fibrosis, vascularization (neo-angiogenesis), and necrosis.<sup>18</sup>

## 2.7 | Statistical analysis

Microbiology statistical analyses were performed with GraphPad Prism software using Mann–Whitney tests. Histological statistical analyses were performed using Kolmogorov–Smirnov tests. The results were expressed as the median  $\pm$  interquartile range (IQR). IQR is the difference between the 75th and 25th percentiles of the data.  $p$ -values were calculated and specified as \* $p < 0.05$ ; \*\* $p < 0.005$ ; \*\*\* $p < 0.001$ ; \*\*\*\* $p < 0.0001$ .

## 3 | RESULTS

### 3.1 | Efficacy study

#### 3.1.1 | Evaluation of the efficacy of DBG21-treated versus untreated titanium implants in a MRSA biofilm murine model

At Day 7 postinoculation, comparable bacterial loads were obtained in control groups (untreated) on implants and surrounding tissues. The median level  $\pm$  IQR of bacterial colonization remained stable over the 14 day-period of infection in the tissues ( $7.18 \pm 1.75 \log_{10}$  CFU/g at D7 and  $6.55 \pm 1.99 \log_{10}$  CFU/g at D14). A slight decrease in the bacterial load was observed on untreated control implants ( $6.51 \pm 0.90 \log_{10}$  CFU at D7 and  $5.84 \pm 1.68 \log_{10}$  CFU at D14); thus, the bacterial colonization was overall quite stable.

At D7 postinoculation, a significant decrease ( $p < 0.0001$ ) in bacterial load was observed in animals that received the DBG21-treated implants, ( $-2.69 \log_{10}$  CFU/g in tissues and  $-3.57 \log_{10}$  CFU on implants). Of note, 3 mice out of 18 (16.6%) had no bacterial growth on their tissues and implants. At D14 postinoculation, this bacterial load decrease was still confirmed, with a more pronounced effect in the surrounding tissues compared to the implant ( $-5.55 \log_{10}$  CFU/g in tissues and  $-1.93 \log_{10}$  CFU on implants) (Figure 1). Of note, 10 out of 14 (71.4%) mice with DBG21-treated discs had no bacterial growth in the surrounding tissues while all of the control mice had bacterial contamination in the surrounding tissues.

### 3.2 | Tolerance study

#### 3.2.1 | Weight and clinical scores

The day following the surgical procedure, mice with treated implants lost 10% of their body weight but regained a weight level at Day 2 comparable to that of animals with untreated control implants. During the 11 days following the subcutaneous implantation, mice gained a similar amount of weight in both the control group and the DBG21-treated group.<sup>19</sup> There was no observed difference in weight between treated and control animals ( $p > 0.05$ ) (Figure 2A). Clinical scores<sup>17</sup> were not statistically different between DBG21-treated and control mice ( $p > 0.05$ ) (Figure 2B). All surgical wounds healed uneventfully.

#### 3.2.2 | Toxicity tests

Eleven days after subcutaneous implantation, no significant biochemical alterations were recorded, regardless of the group (control or treated). No statistically significant differences between groups were observed ( $p > 0.05$ ) (Figure 2C).

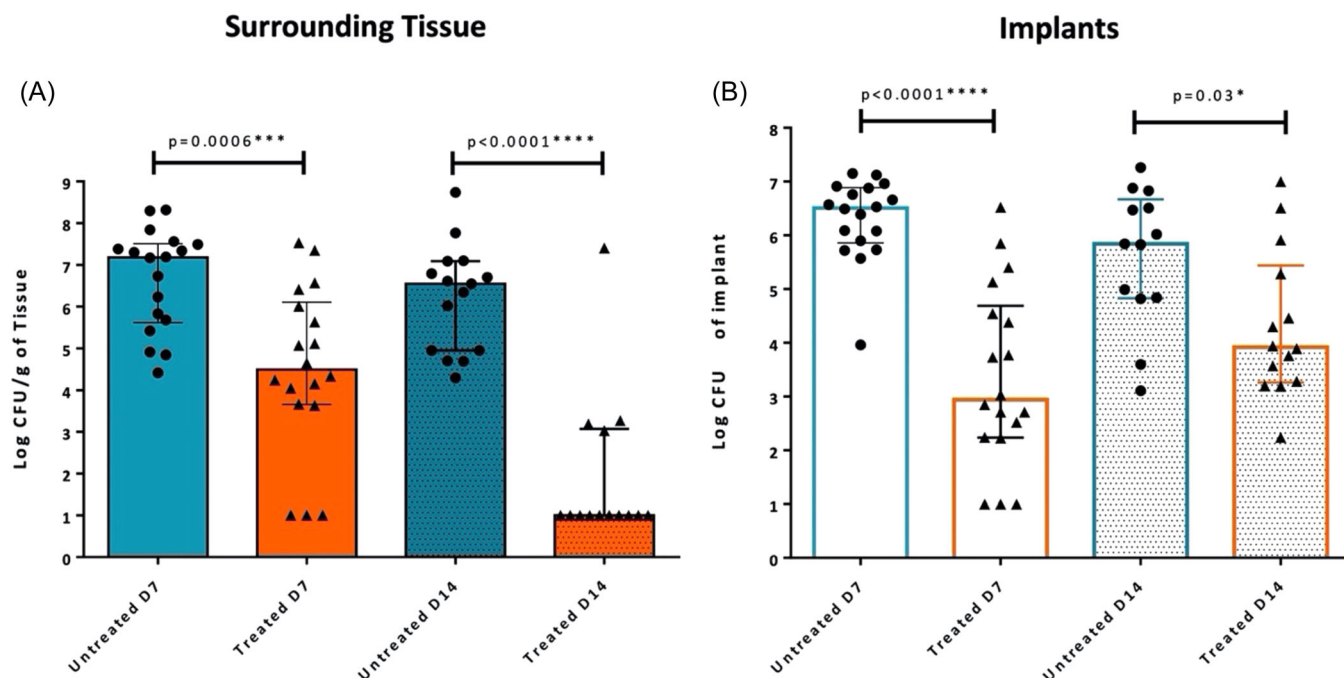


**FIGURE 1** Antibacterial efficacy of DBG21-treated titanium implants versus controls against methicillin-resistant *Staphylococcus aureus* (MRSA) (ATCC 43300) biofilm in a mouse model of implant-associated infection after 7 and 14 days of infection in surrounding tissues (A) and on implants (B).

### 3.2.3 | Impact of DBG21-treated implants on local toxicity

Representative pictures of the implant cavity with surrounding tissues in untreated mice and treated mice are displayed respectively in Figure 3A,B. A side-by-side photographic comparison between a control and a treated mouse is shown in Figure 3C. After 11 days of subcutaneous implantation, the microscopic analysis of the HES-stained slides showed no significant cytological alterations, no increased fibrosis or inflammation, and no necrosis or neo-angiogenesis in the treated group versus controls ( $p > 0.05$ ).

## 3.3 | Pathology study

### 3.3.1 | Histopathological impact of DBG21-treated implants versus untreated titanium-alloy implants on surrounding tissues in an MRSA biofilm model

The use of treated implants trended toward decreased inflammation, fibrosis, vascularization, and necrosis rates at D7 and D14 post-implantation, as seen in Figure 4 ( $p > 0.05$ ). These results indicate that in the presence of an infection, DBG21-treated implants did not generate suppurative and necrotic inflammation over time, unlike control implants with the same bacterial inoculum. The analysis over the 2-week study time period of either control or DBG21-treated implant effects did not have any significant differences between the two time points. As observed in Figure 4, the presence of

inflammation, fibrosis, vascularization, and necrosis on D7 persisted until D14 for control implants.

## 4 | DISCUSSION

Data from the American Joint Replacement Registry showed that infection is the number one cause of early and late failure for both hip and knee replacement.<sup>20</sup> Despite best efforts of prevention, the number of primary hip and knee replacement leading to infection is still on the rise and affects patient quality of life, risk of infection recurrence, amputation, and death. In this *in vivo* study, we demonstrated that a novel covalently grafted antimicrobial compound significantly decreased MRSA growth both on a titanium disc and in the surrounding soft tissues. Moreover, our finding also indicates the absence of local and systemic toxicity. High bacterial median  $\log_{10}$  reductions on implants were achieved at both 7 and 14 days postoperatively despite the use of a high inoculum, the absence of antibiotics, and the use of a virulent strain with known capability to adhere to biomaterials (MRSA). Furthermore, the bacterial reductions observed in the soft tissues improved with time between Day 7 and Day 14. DBG21-treated implants did not induce any acute or subacute systemic toxicity in mice (ISO 10993-11:2017<sup>17</sup>). The histopathological analysis revealed no differences in local toxicity between the treated and control groups. Taken together, these findings strongly support an excellent biocompatibility profile of DBG21-treated titanium implants.

In this investigation, given that the compound was designed to be noneluting, one may hypothesize that the strong biofilm inhibition



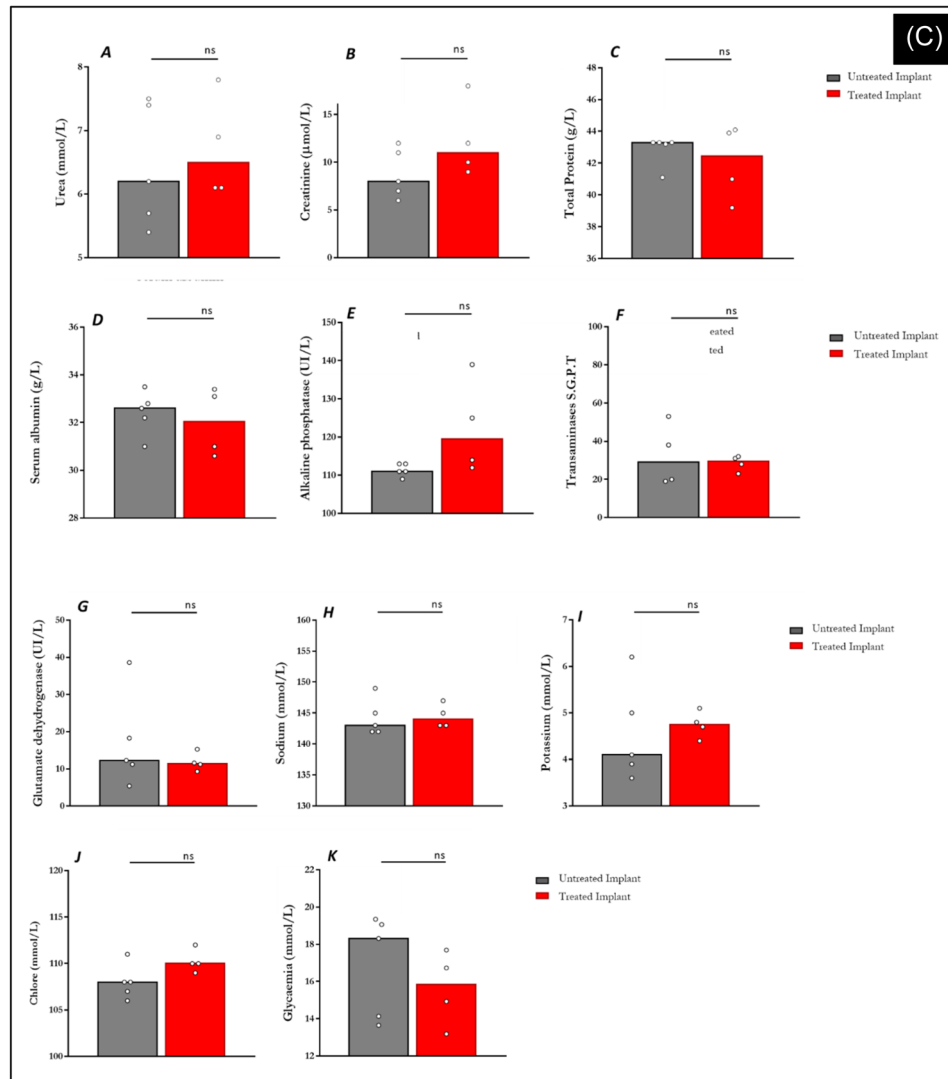
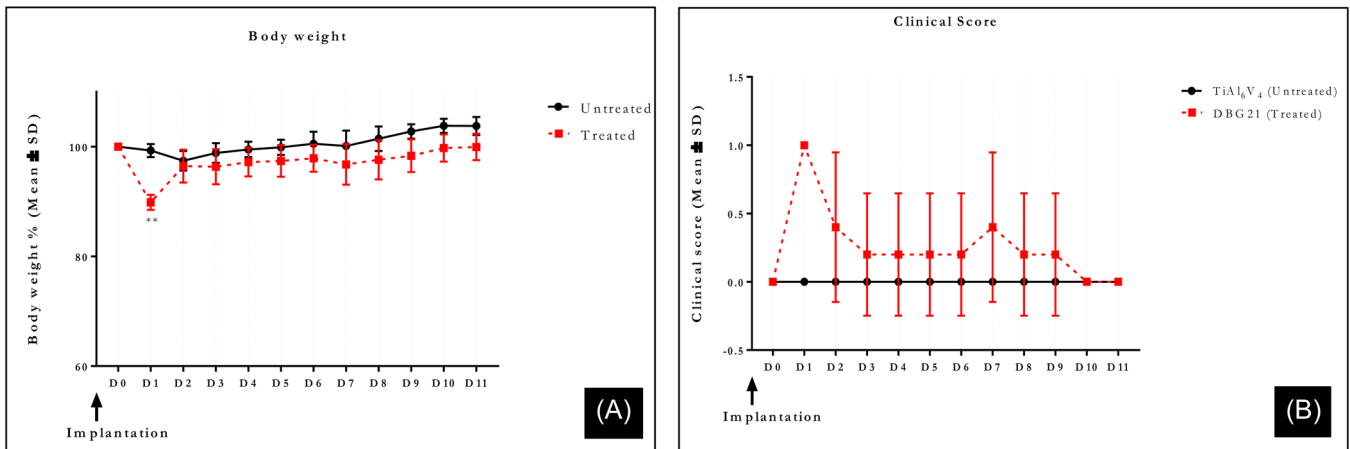


**FIGURE 2** (A) Body weight measurement (expressed as % body weight, mean ± SD) in DBG21-treated and untreated mice up to 11 days postimplantation. (B) Clinical scores (expressed as % body weight, mean ± SD) in DBG21-treated and untreated mice up to 11 days postimplantation. (C) Biochemical assessment (median is presented) from animals receiving untreated or DBG21-treated implants at D11 postimplantation. (A): Urea, B: Creatinine, C: Total Protein, D: Serum albumin, E: Alkaline Phosphatase, F: Transaminases S.G.P.T, G: Glutamate dehydrogenase, H: Sodium, I: Potassium, J: Chlore, K: Glycaemia).

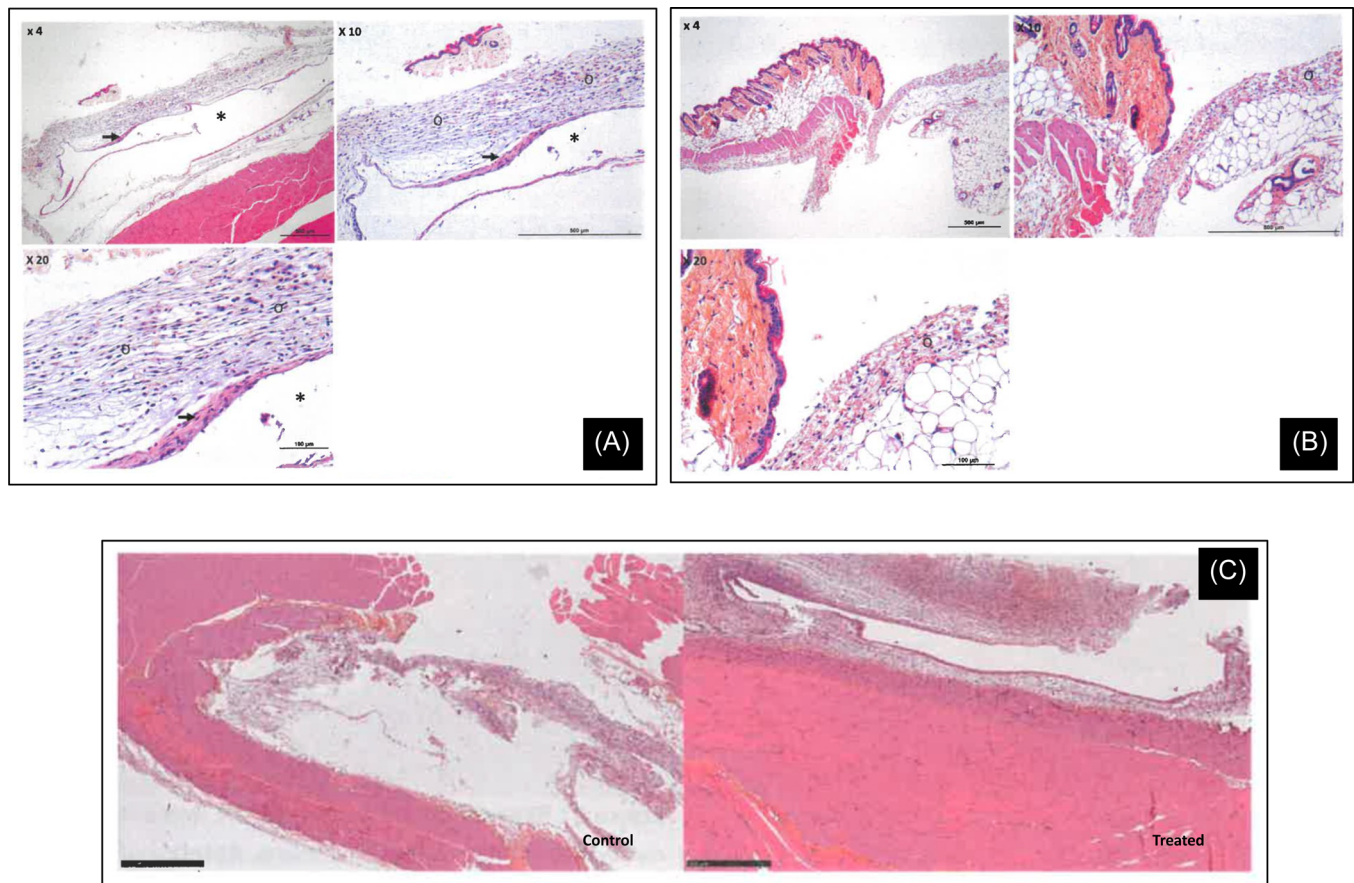


**FIGURE 3** (A) Representative picture of the implant cavity with different magnifications. Presence of an optically empty cavity (\*) in the subcutaneous adipose-connective location, circumscribed by a light fibrous densification (arrow). Slight leukocytic densification in the loose connective tissue at the periphery of the polymorphic cavity, predominantly mononuclear (o). (B) Representative picture of the implant cavity with different magnifications. Absence of cavitary lesion in the subcutaneous connective tissue. Minimal leukocyte densification in loose, predominantly mononuclear connective tissue (o). (C) Representative pictures of the implant tolerance. Left panel: sample previously with neutral titanium implant. Right panel: sample previously with treated titanium implant.

allowed the immune response to build over time and clear bacteria in the surrounding soft tissues. These findings have to be interpreted in light of the context: a stringent model using a high MRSA inoculum ( $1 \times 10^7$  CFU) with direct injection into the operative site after skin closure in the absence of perioperative antibiotics. This surpasses almost all scenarios of surgical contamination as it was demonstrated based on experimental animal data that approximately  $10^2$  CFU of *S. aureus* are sufficient to establish infection if inoculated at the time of a hip hemiarthroplasty in a rabbit model.<sup>21</sup> Moreover, despite the smaller sample size of the histopathological efficacy substudy, there was demonstrated decreased inflammation, fibrosis, vascularization, and necrosis around the treated versus control discs. In the presence of infection, all these positive findings (bacterial counts and histopathological analysis) showed that DBG21-treated discs were able to mitigate infection, or even bring the infection under control in some of the mice, despite a high MRSA bacterial load and without the use of antibiotics.

Comparison of the bacterial reductions on titanium implants between DBG21 and data from previously published peer-reviewed

studies (Table 2) showed that the current study had one of the longest (14 days) time periods of observation after MRSA inoculation. The bacterial reductions reported on implants and in the surrounding tissues in the present study outperformed the scientific literature on comparable subcutaneous infection rodent models with titanium implants. Indeed, most published studies do not exceed 2.5–2.75  $\log_{10}$  bacterial reductions both in the surrounding tissues and on implants for bacterial strains with less virulence (*Staphylococcus epidermidis*), lower inoculum (6  $\log_{10}$  and below), and shorter time points (under 7 days). Also, most of the processes described in the literature are exceedingly complex, requiring the use of toxic reagents and/or solvents, and do not meet standards of scalability in the orthopaedic industry.

Interestingly, the bacterial log reductions observed in our study in the surrounding tissue that improved between Days 7 and 14 were not found in the literature pertaining to covalently bound antimicrobials.<sup>9,10</sup> Typically, authors reported no reduction of bacterial growth in surrounding tissues for covalently bound antimicrobials. This could be due to their lower bactericidal effect on contact and thus lower biofilm inhibition since biofilm and tissue



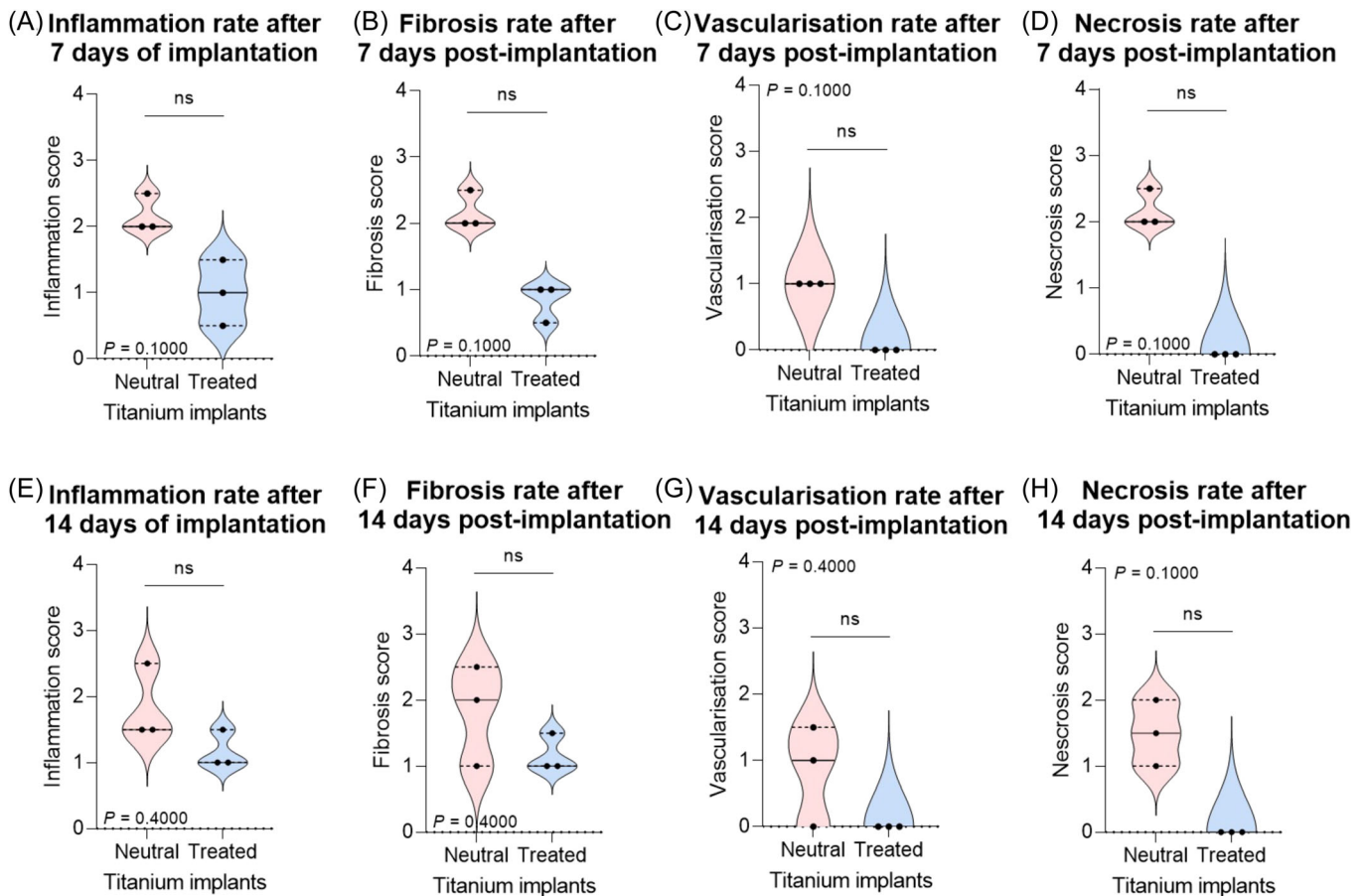


**FIGURE 4** Description of the effect of titanium implants + bacterial inoculum on the adjacent tissues at two timepoints (D7 and D14). (A–D) Results observed after 7 days of implantation. (E–H) Results after 14 days of implantation. (A, E) Inflammation rate. (B, F) Fibrosis rate. (C, G) Angiogenesis rate. (D, H) Necrosis rate.

**TABLE 2** Comparative data for various antibacterial surface technologies.

Authors	Technology	Strain	Animals	N	Inoc.	BTP	MR	Duration (days)
Hashimoto et al. <sup>11</sup>	HA/Silver coating	MRSA	Rats	12	6	1	0.35	1
Ueno et al. <sup>13</sup>	HA/Silver coating	MRSA	Rats	10	8	7	0.41	7
Shimazaki et al. <sup>12</sup>	HA/Silver coating	MRSA	Rats	10	6	3	1.4	3
Gerits et al. <sup>10</sup>	Covalent SPI031	MRSA	Mice	26	7	4	1.7	4
Chen et al. <sup>7</sup>	Melimine peptide coating	MRSA	Rats	34	5	5	2	7
Kucharikova et al. <sup>9</sup>	Covalent Vancomycin	MSSA	Mice	19	7	4	2.5	4
Skovdal et al. <sup>6</sup>	Ultradense PEG coating	<i>Staphylococcus epidermidis</i>	Mice	31	9	5	2.75	5
Tilmaciu et al. <sup>8</sup>	Covalent Ag-loaded phosphonates	<i>S. epidermidis</i>	Mice	10	4	14	3.6	14
Current study	Covalent high-density quaternary ammonium polymer (proprietary)	MRSA	Mice	65	7	7	3.6	14

Abbreviations: BTP, best time points (days); HA, hydroxyapatite; Inoc., inoculum (Log<sub>10</sub> CFU); MR, max reduction (Log<sub>10</sub> CFU); MRSA, methicillin-resistant *Staphylococcus aureus*; PEG, polyethylene glycol.

bacterial burden are not two separate entities but are interdependent mechanisms. As was shown over 60 years ago by Elek et al.,<sup>22</sup> it is the presence of the foreign body that allows the infection to persist despite a low inoculum.

Our investigation has some limitations. First, the antibacterial effect was more pronounced on treated implants at D7 than D14. This is most likely related to a limitation of the model to perform true bacterial enumeration on implants at Day 14. A capsule

formed on several discs at Day 14 in the presence of infection, which is a limitation of the animal model used. Because of this protocol, the capsule cannot be removed to count bacteria on the titanium surface. Therefore, the bacterial reduction described at Day 14 reflects what occurred either on the titanium surface or on a capsule, based on the amount of tissue response in the presence of infection. Interestingly, the soft tissues demonstrated no bacterial growth in most mice in the same timeframe. What occurs on the surface of the titanium after Day 14 remains an open question and most likely cannot be answered using this model. Indeed, bacteria are still detectable around peri-implant capsules in all mice at Day 14. The clinical impact is expected to be different as the standard treatment of implant-related infections involves the use of intravenous antibiotics, which were intentionally withheld from this animal trial to elucidate the specific role of DBG21. Indeed, antibiotics are known to be synergistic with antimicrobial surface technologies.<sup>6</sup> Second, we acknowledge that this small animal trial does not provide data regarding bone ingrowth in contact with the implant. A large animal trial is planned to provide data on efficacy in a bone-relevant model and on osseointegration, which is clinically paramount. This trial was designed as an initial proof of concept for antimicrobial surface modification of medical devices, not solely for orthopedic applications, as titanium-alloy is a gold-standard metal for numerous other medical applications. Small animal models also allow the collection of more complete safety and efficacy data with the use of larger sample sizes. Third, we acknowledge the low sample size in the safety study. We found no histological differences between treated and control in the absence of infection. Moreover, our findings are consistent with Schaer et al.<sup>23</sup> whose team studied a different quaternary ammonium polymer (N,N-dodecylmethyl-PEI coatings) on locking compression plates for tibial osteotomies in sheep. They found that their coating neither negatively impacted soft or calcified tissue physiology nor altered the healing response over at least a 3-month period. Schaer et al. also found less in vivo inflammation in the setting of infection on treated implants versus controls, which is in agreement with our study findings. Last, the present study was performed with MRSA only and further in-vivo studies are warranted to investigate the efficacy on other bacterial strains. Because quaternary ammonium polymers are already known to eliminate both gram-positive and gram-negative bacteria in vitro and in vivo,<sup>24</sup> similar findings could be possible in further DBG21 studies.

Aside from cost, the treatment of implant-related and periprosthetic joint infections demands a minimum 6-week exposure to systemic antibiotics for the patient. These prolonged antibacterial treatments commonly cause profound microbiota disturbance producing gastrointestinal symptomatology and convey risk of both superimposed *Clostridioides difficile* colonic infection and drug-induced allergic reaction. Because treatment is often intravenous, catheter complications such as deep venous thrombosis and central line-associated bloodstream infection (CLA-BSI) are inherent risks.

## 5 | CONCLUSION

Overall, these results showed that the MRSA biofilm was reduced by up to 99.97% in mice that received DBG21-treated titanium-alloy implants compared to untreated control implants without causing measurable toxicity. This level of protection provided by a noneluting surface treatment despite a high bacterial inoculum of a virulent strain is novel and has the potential to prevent implant-related infections in humans.

## AUTHOR CONTRIBUTIONS

*Substantial contributions to research design, or the acquisition, analysis, or interpretation of data:* Houssam Bouloussa, Othman Bouloussa, Mohsin Mirza, Azzam Saleh-Mghir, Bradley Stutzman, Claudio Vergari, Nelson Anzala, Dorian Bonnot, Sandrine Albac, Delphine Croisier. *Drafting the paper or revising it critically:* Houssam Bouloussa, Emmanuel Gibon, Zoe Durand, Antonia F. Chen, Matthew Grant, James Yue. *Approval of the submitted and final versions:* Houssam Bouloussa, Emmanuel Gibon, Antonia F. Chen, Matthew Grant.

## ACKNOWLEDGMENTS

Houssam Bouloussa, Zoe Durand, Emmanuel Gibon, and Othman Bouloussa are DeBogey Molecular, Inc. founders and shareholders.

## ORCID

Emmanuel Gibon  <http://orcid.org/0000-0002-4049-1831>

Antonia F. Chen  <http://orcid.org/0000-0003-2040-8188>

Claudio Vergari  <http://orcid.org/0000-0002-7049-2405>

## REFERENCES

- Zmistowski B, Karam JA, Durinka JB, Casper DS, Parvizi J. Periprosthetic joint infection increases the risk of one-year mortality. *J Bone Joint Surg.* 2013;95-24:2177-2184.
- Kurtz SM, Lau E, Watson H, Schmier JK, Parvizi J. Economic burden of periprosthetic joint infection in the United States. *J Arthroplasty.* 2012;27:61-65.
- Urish KL, DeMuth PW, Kwan BW, et al. Antibiotic-tolerant *Staphylococcus aureus* biofilm persists on arthroplasty materials. *Clin Orthop Rel Res.* 2016;474:1649-1656.
- Saeed K, McLaren AC, Schwarz EM, et al. International consensus meeting on musculoskeletal infection: summary from the biofilm workgroup and consensus on biofilm related musculoskeletal infections. *J Orthop Res.* 2018;2019(37):1007-1017.
- Alt V, Chen AF. Antimicrobial coatings for orthopaedic implants-ready for use? *J Bone Jt Infect.* 2020;5:125-127.
- Skovdal SM, Jørgensen NP, Petersen E, et al. Ultra-dense polymer brush coating reduces *Staphylococcus epidermidis* biofilms on medical implants and improves antibiotic treatment outcome. *Acta Biomater.* 2018;76:46-55.
- Chen R, Willcox MDP, Ho KKK, Smyth D, Kumar N. Antimicrobial peptide melimine coating for titanium and its in vivo antibacterial activity in rodent subcutaneous infection models. *Biomaterials.* 2016; 85:142-151.
- Tilmaçiu C-M, Mathieu M, Lavigne J-P, et al. In vitro and in vivo characterization of antibacterial activity and biocompatibility: a study on silver-containing phosphonate monolayers on titanium. *Acta Biomater.* 2015;15:266-277.

9. Kuchariková S, Gerits E, De Brucker K, et al. Covalent immobilization of antimicrobial agents on titanium prevents *Staphylococcus aureus* and *Candida albicans* colonization and biofilm formation. *J Antimicrob Chemother.* 2016;71:936-945.
10. Gerits E, Kuchariková S, Van Dijck P, et al. Antibacterial activity of a new broad-spectrum antibiotic covalently bound to titanium surfaces. *J Orthop Res.* 2016;34:2191-2198.
11. Hashimoto A, Miyamoto H, Kobatake T, et al. The combination of silver-containing hydroxyapatite coating and vancomycin has a synergistic antibacterial effect on methicillin-resistant *Staphylococcus aureus* biofilm formation. *Bone Joint Res.* 2020;9-5: 211-218.
12. Shimazaki T, Miyamoto H, Ando Y, et al. In vivo antibacterial and silver-releasing properties of novel thermal sprayed silver-containing hydroxyapatite coating. *J Biomed Mater Res B Appl Biomater.* 2010; 92:386-389.
13. Ueno M, Miyamoto H, Tsukamoto M, et al. Silver-containing hydroxyapatite coating reduces biofilm formation by methicillin-resistant *Staphylococcus aureus* in vitro and in vivo. *BioMed Res Int.* 2016;20168070597. doi:10.1155/2016/8070597
14. Ravanetti F, Chiesa R, Ossiprandi M, et al. Osteogenic response and osteoprotective effects in vivo of a nanostructured titanium surface with antibacterial properties. *J Mater Sci Mater Med.* 2016;27-3: 1-15.
15. Chouirfa H, Bouloussa H, Migonney V, Falentin-Daudré C. Review of titanium surface modification techniques and coatings for antibacterial applications. *Acta Biomater.* 2019;83:37-54.
16. Tasse J, Croisier D, Badel-Berchoux S, et al. Preliminary results of a new antibiotic susceptibility test against biofilm installation in device-associated infections: the antibiofilmogram®. *Pathog Dis.* 2016;74:ftw057.
17. ISO. ISO 10993-11:2017(en), *Biological Evaluation of Medical Devices—Part 11: Tests for Systemic Toxicity.* ISO.
18. Ozgol I, Depboylu BC, Tongut A, et al. Evaluation of infection resistance of biodegradable versus conventional annuloplasty rings in an in vivo rat subcutaneous model. *Eur Surg Res.* 2017;58:169-179.
19. River C. BALB/c Mice | Charles River. 2023. <https://www.criver.com/products-services/find-model/balbc-mouse?region=29>
20. Springer BD, Cahue S, Etkin CD, Lewallen DG, McGroarty BJ. Infection burden in total hip and knee arthroplasties: an international registry-based perspective. *Arthroplast Today.* 2017;3:137-140.
21. Southwood R, Rice J, McDonald P, Hakendorf P, Rozenbils M. Infection in experimental hip arthroplasties. *J Bone Joint Surg Br.* 1985;67-B:229-231.
22. Elek SD, Conen P. The virulence of *Staphylococcus pyogenes* for man. A study of the problems of wound infection. *Br J Exp Pathol.* 1957;38-6:573.
23. Schaer TP, Stewart S, Hsu BB, Klibanov AM. Hydrophobic polycationic coatings that inhibit biofilms and support bone healing during infection. *Biomaterials.* 2012;33:1245-1254.
24. Kamaruzzaman NF, Tan LP, Hamdan RH, et al. Antimicrobial polymers: the potential replacement of existing antibiotics? *Int J Mol Sci.* 2019;20:2747.

**How to cite this article:** Bouloussa H, Durand Z, Gibon E, et al. A novel antibacterial compound decreases MRSA biofilm formation without the use of antibiotics in a murine model. *J Orthop Res.* 2023;1-10. doi:10.1002/jor.25638